

Resonant three-dimensional photonic crystals

E.L. Ivchenko and A.N. Poddubny

A.F. Ioffe Physico-Technical Institute, Russian Academy of Sciences, St. Petersburg 194021, Russia

We have developed a theory of exciton-polariton band structure of resonant three-dimensional photonic crystals for arbitrary dielectric contrast and effective mass of the exciton that is excited in one of the compositional materials. The calculation has been carried out for a periodic array of spheres embedded in a dielectric matrix. It has been shown that the position of the lower branches of the polariton dispersion curve monotonously depends on the exciton effective mass and is determined by the coupling of light with the first few states of the mechanical exciton quantum confined inside each sphere. Particularly, we have studied the role of excitonic effects on the photonic-crystal band gap along the [001] direction of the Brillouin zone and presented an analytic description of the polariton dispersion in terms of the two-wave approximation.

PACS numbers: 71.35.-y, 71.36.+c, 42.70.Qs

1. INTRODUCTION

The concept of photonic crystals was put forward by Yablonovich¹ and John² in 1987. Since then this term is used for media with the dielectric susceptibility varying periodically in the space and allowing the Bragg diffraction of the light. The theory of photonic crystals has been developed in a number of subsequent works, see, e.g., Refs. 3,4,5,6,7. The main goal of these studies was to determine the photon band structure and analyze the sequence of allowed bands and stop-bands (gaps) for different directions of the wave vector in the first Brillouin zone. The simplest model realization of a photonic crystal is a structure grown from two materials, A and B, with different dielectric constants ε_A and ε_B : a periodic layered medium ...A/B/A/B... in case of *one-dimensional* photonic crystals and periodic arrays of cylinders and spheres of the material A embedded in a dielectric matrix B, in case of *two-dimensional* and *three-dimensional* photonic crystals, respectively. Periodic structures where the dielectric susceptibility of one of the compositional materials, as a function of the frequency ω , has a pole at a certain resonance frequency are grouped into a special class of resonant photonic crystals. In such systems the normal light waves are excitonic polaritons. In Refs. 8,9 the dispersion of light waves has been calculated taking into consideration the frequency dependence of the dielectric susceptibility in the frame of the local material relation $\mathbf{D} = \varepsilon_A(\omega)\mathbf{E}$ between the electric displacement and the electric field. In Ref. 10 the dispersion of excitonic polaritons in a resonant photonic crystal has been calculated taking into account only one level of the quantum-confined exciton in a sphere A and neglecting the difference between the dielectric constant ε_B and the background dielectric constant ε_a of the material A. In the present work we have studied theoretically the dispersion of excitonic polaritons in a resonant photonic crystal making allowance for all available exciton quantum-confinement levels as well as for the dielectric contrast, i.e., for $\varepsilon_a \neq \varepsilon_B$.

2. PROBLEM DEFINITION AND METHOD OF CALCULATION

In this work the theory of resonant photonic crystals is developed for a periodic array of spheres A arranged in a face-centered cubic (FCC) lattice and embedded in the matrix B. The structure under consideration is characterized by seven parameters: R , a , ε_B , ε_a , ω_{LT} , ω_0 and M . Here R is the radius of the spheres A, a is the lattice constant for the FCC lattice, ε_B is the dielectric constant of the matrix, ω_0 , ω_{LT} and M are the resonance frequency, longitudinal-transverse splitting and translational effective mass of the triplet $1s$ exciton excited inside the spheres A, ε_a is the background dielectric constant that contains contributions to the dielectric response from all other electron-hole excitations. Thus, we assume the dielectric function of the bulk material A to have the form

$$\varepsilon_A(\omega, \mathbf{q}) = \varepsilon_a + \frac{\varepsilon_a \omega_{LT}}{\omega_{exc}(\mathbf{q}) - \omega}, \quad \omega_{exc}(\mathbf{q}) = \omega_0 + \frac{\hbar q^2}{2M} \quad (1)$$

and, in that way, take into account both the frequency and spatial dispersion, i.e. the dependence on the light frequency ω and wave vector \mathbf{q} . The radius R is chosen so that, on the one hand, the spheres A do not overlap, i.e. $R < a/2\sqrt{2}$, but, on the other hand, R should exceed the Bohr radius of the $1s$ -exciton in the material A and, hence, the exciton can be considered as a single particle with the mass M . In the following we ignore the frequency dependence of the parameters ε_B and ε_a . Moreover, hereafter we assume the material A to be isotropic and take into consideration the bulk $1s$ exciton states only. It follows then that the problem is reduced to the solution of a system of two vector equations, namely, the wave equation

$$\text{rot rot } \mathbf{E}(\mathbf{r}) = \left(\frac{\omega}{c}\right)^2 [\varepsilon(\mathbf{r})\mathbf{E}(\mathbf{r}) + 4\pi\mathbf{P}_{exc}(\mathbf{r})] \quad (2)$$

and the material equation for the $1s$ -exciton contribution to the dielectric polarization

$$\left(-\frac{\hbar}{2M} \Delta + \omega_0 - \omega\right) \mathbf{P}_{exc}(\mathbf{r}) = \frac{\varepsilon_a \omega_{LT}}{4\pi} \mathbf{E}(\mathbf{r}), \quad (3)$$

where $\varepsilon(\mathbf{r}) = \varepsilon_a$ inside the spheres and $\varepsilon(\mathbf{r}) = \varepsilon_B$ outside the spheres, $\mathbf{E}(\mathbf{r})$ and $\mathbf{P}_{\text{exc}}(\mathbf{r})$ are the electric field and the excitonic polarization at the frequency ω . On a spherical surface separating materials A and B we impose the standard Maxwell boundary conditions: continuity of the tangential components of the electric and magnetic fields, and the Pekar additional boundary condition for the excitonic polarization: the vanishing vector $\mathbf{P}_{\text{exc}}(\mathbf{r})$ at $|\mathbf{r} - \mathbf{a}| = R$, where the translational vectors \mathbf{a} define the centers of spheres A.

Due to the periodicity of the structure we can seek solutions of Eqs. (2) and (3) in the Bloch form satisfying the condition

$$\mathbf{E}_{\mathbf{k}}(\mathbf{r} + \mathbf{a}) = e^{i\mathbf{k}\mathbf{a}} \mathbf{E}_{\mathbf{k}}(\mathbf{r}). \quad (4)$$

Here \mathbf{k} is the exciton-polariton wave vector defined within the first Brillouin zone. We remind that, for a FCC lattice, the latter is a dodecahedron bounded by six squares and eight hexagons.

Below we present the results of calculation of the exciton-polariton dispersion $\omega_{n\mathbf{k}}$, where n is the branch index. The computation was mainly performed by using a photon analogue of the Korringa-Kohn-Rostoker (KKR) method^{11,12,13}. In this method (i) the electric field is decomposed in the spherical waves, or more precisely, in the vector spherical functions centered at the points $\mathbf{r} = \mathbf{a}$, and (ii) following the consideration of the light scattering by a single sphere and the introduction of a structural factor the dispersion equation is transformed to

$$|\delta_{j'j} \delta_{m'm} \delta_{\sigma'\sigma} - G_{j'm'\sigma',jm\sigma}(\mathbf{k}, \omega) R_{j\sigma}(\omega)| = 0. \quad (5)$$

Here $R_{j\sigma}$ are the coefficients describing the scattering of spherical waves by a single sphere A, they depend on the total angular momentum j and the polarization index σ discriminating the magnetic and electric spherical harmonics but are independent of the angular-momentum component m . Note that, for a spherical scatterer, these coefficients relate the incident field $\mathbf{E}_0(\mathbf{r}) \propto \mathbf{J}_{jm\sigma}(\mathbf{r})$ with the scattered field $\mathbf{E}_{\text{sc}}(\mathbf{r}) \propto \mathbf{H}_{jm\sigma}(\mathbf{r})$, where $\mathbf{J}_{jm\sigma}, \mathbf{H}_{jm\sigma}$ are the vector spherical functions¹³. Ajiki et al.¹⁴ have calculated values of $R_{j\sigma}(\omega)$ taking into account the exciton resonance in the spheres A and the finite exciton effective mass M . In contrast to the scattering matrix for a single sphere which is diagonal, $R_{j'm'\sigma',jm\sigma} \equiv R_{j\sigma} \delta_{j'm'\sigma',jm\sigma}$, the matrix of structural factors $G_{j'm'\sigma',jm\sigma}(\mathbf{k}, \omega)$ has nonvanishing diagonal and off-diagonal components. It should be mentioned that the both matrices are frequency dependent whereas only the structural matrix \mathbf{G} depends upon the polariton wave vector \mathbf{k} . At the same time \mathbf{G} is independent of the excitonic parameters and coincides with the matrix considered in Refs. 11,12,13 where the exciton states are disregarded.

In addition to the KKR method, in section 4 we apply the Green-function technique for the analysis of separate contributions of quantum-confined excitonic levels to the

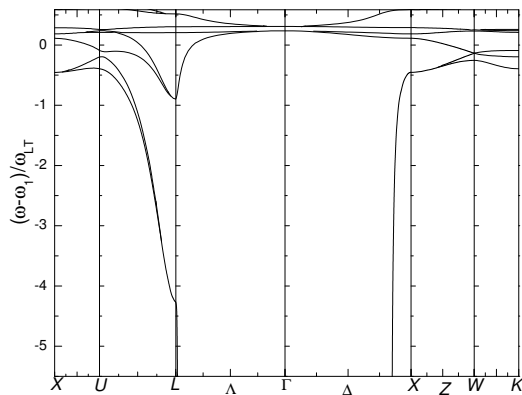


FIG. 1: Exciton-polariton band structure of a photonic crystal with a FCC lattice of spheres A inserted into the matrix B. The calculation is performed neglecting the dielectric contrast and for the set of parameters indicated in the text.

polariton dispersion, and in section 5 we use the two-wave approximation which allows an analytic description.

3. POLARITON DISPERSION FOR A FINITE EXCITON MASS

First we focus the attention upon purely excitonic effects and neglect the dielectric contrast assuming $\varepsilon_a = \varepsilon_B$. Then in the absence of exciton-photon interaction, i.e. for $\omega_{\text{LT}} = 0$, the medium becomes optically homogeneous and photons propagating therein are characterized by the linear dispersion $\omega = cq/n_B$ with the refractive index $n_B = \sqrt{\varepsilon_B}$. In the reduced zone scheme, this single-valued relation between the frequency and wave vector \mathbf{q} turns into the many-valued (or multi-branch) dispersion curve

$$\omega_{\mathbf{k}} = c|\mathbf{k} + \mathbf{b}|/n_B, \quad (6)$$

where \mathbf{b} is the reciprocal lattice vector reducing \mathbf{q} to the vector $\mathbf{k} = \mathbf{q} - \mathbf{b}$ that lies in the first Brillouin zone. A nonvanishing value of ω_{LT} leads to a mixing between photonic and excitonic states and formation of hybrid polariton excitations characterized by a complicated multiband dispersion $\omega_{n\mathbf{k}}$. As a result the wave (n, \mathbf{k}) is a mixture of two or more photonic states (6) with the same \mathbf{k} but different \mathbf{b} .

Fig. 1 presents the dispersion of exciton-polaritons calculated for a FCC lattice and the following set of structure parameters:

$$\varepsilon_a = \varepsilon_B = 10, R = a/4, \hbar\omega_1 = 2 \text{ eV}, \omega_{\text{LT}} = 5 \times 10^{-4} \omega_1,$$

$$P \equiv \left(\frac{\sqrt{3}\pi c}{\omega_1 n_B a} \right)^3 = 1.1, M = 0.5 m_0.$$

Here m_0 is the free electron mass in vacuum and, instead

of the bulk exciton resonance frequency ω_0 , we introduced the resonance frequency

$$\omega_1 = \omega_0 + \frac{\hbar}{2M} \left(\frac{\pi}{R}\right)^2 \quad (7)$$

of the ground state of the exciton quantum-confined in a sphere of the radius R . Note that, for the structure tuned to the Bragg resonance $\omega_1 = ck_L/n_b$ at the point L of the Brillouin zone with $k_L = \sqrt{3}\pi/a$ or $\omega_1 = ck_X/n_b$ at the point X with $k_X = 2\pi/a$, the parameter P equals to 1 and $3\sqrt{3}/8 \approx 0.65$, respectively. For $P = 1.1$, the anticrossing between the horizontal line $\omega = \omega_1$ (“bare” exciton branch) and the line $\omega = ck/n_B$ (“bare” photon branch) occurs inside the Brillouin zone at k amounting approximately 97% of k_L and 84% of k_X . For the sake of completeness the dependence $\omega(\mathbf{k})$ is shown not only along the high-symmetry crystallographic directions $\mathbf{k} \parallel [001]$ (points Δ) and $\mathbf{k} \parallel [111]$ (points Λ) but also along the straight lines $X - W$, $W - K$, $X - U$ and $U - L$.

In Fig. 1 the frequency region is cut from above in order to keep only few branches of the dispersion curve. In the cut region the dispersion is presented by a dense network of polariton branches which appear as a result of the anticrossing of “bare” photonic branches (6) with a set of close-lying exciton quantum-confinement levels. The network has a tangled character complicated for depiction. Therefore, we concentrate here on the analysis of the role played by the photonic-crystal parameters in the formation of the lower polariton branches.

In Fig. 2 the solid curves show the same dispersion branches as in the previous figure but in an increased scale and in the vicinity of the points X and L . For comparison we also present, by dashed-and-dotted lines, the lower branch of the dispersion curve calculated taking into account only the ground exciton quantum-confinement level. The calculation was performed by reducing the value of M to $0.01m_0$ and decreasing ω_0 so that the frequency ω_1 in Eq. (7) was kept invariant. The dashed-and-dotted lines coincide with those calculated by the method proposed for exciton-polaritons in Ref. 10. Dashed curves illustrate the opposite limiting case of quite heavy excitons, $M \rightarrow \infty$. In this case the relation between the exciton polarization and electric field becomes local:

$$\mathbf{P}_{\text{exc}} = \chi \mathbf{E}, \quad \chi = \frac{\varepsilon_a}{4\pi} \frac{\omega_{\text{LT}}}{\omega_0 - \omega}.$$

It means that values of \mathbf{k} corresponding to a certain frequency ω can be found in the same way as it is done for nonresonant photonic crystal with the dielectric susceptibilities ε_B and $\varepsilon_A = \varepsilon_a + 4\pi\chi$. The calculation shows that the dashed line in Fig. 2 is practically indistinguishable from the lower branch obtained according to Eq. (5) for $M = 5m_0$. The lower polariton branch is formed as a result of “repulsion” of the photon branch (6) with $\mathbf{b} = 0$ towards the long-wavelength side because of the interaction with the exciton quantum-confinement levels. For

$M \rightarrow 0$ but $\omega_1 = \text{const}$, this branch is remarkably affected by the lower level (7) only. For $M \rightarrow \infty$, the

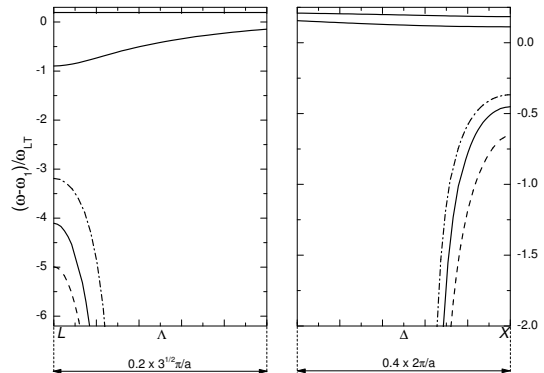


FIG. 2: Dispersion of exciton polaritons in a resonant photonic crystal in the spectral region adjoining the resonance frequency of the lower exciton level ω_1 and for the wave vectors $\mathbf{k} \parallel [111]$ (points Λ) and $\mathbf{k} \parallel [001]$ (points Δ). The dispersion curves are calculated for the exciton effective mass $M = 0.5m_0$ (solid lines), $M \rightarrow \infty$ (dashed lines) and $M \rightarrow 0$ (dashed-and-dotted lines). Other parameters are the same as in Fig. 1.

other levels act upon this branch to the maximum since in this limit their resonance frequencies coincide and are equal to ω_0 . We conclude then that the lower polariton branch corresponding to the finite mass M must always lie between the dashed-and-dotted and dashed lines, in agreement with the results of calculation shown in Fig. 2.

4. COMPARATIVE CONTRIBUTION OF INDIVIDUAL QUANTUM-CONFINED EXCITON LEVELS

In the following we use the notation $\omega_X(M)$ for the frequency at the X point in the lowest polariton branch for the exciton effective mass M in the material A, $\omega_X(0)$ and $\omega_X(\infty)$ for values of this frequency for $M \rightarrow 0$ and $M \rightarrow \infty$, and, finally, $\bar{\omega}_X$ for the arithmetic mean $[\omega_X(0) + \omega_X(\infty)]/2$. One can see from Fig. 2 that the difference $\omega_1 - \bar{\omega}_X$ noticeably exceeds the difference $\omega_X(0) - \omega_X(\infty)$. This means that the main contribution to the position of the frequency $\omega_X(M)$ should come from the exciton-photon coupling with the ground level (7). In this section we analyze in detail the influence of the ground and excited levels of the quantum-confined exciton on the lower polariton branch. To this end we follow Ref. 14, use the Green-function technique and expand a solution of equation (3) with arbitrary function $\mathbf{E}(\mathbf{r})$ in a series

$$\mathbf{P}_{\text{exc}}(\mathbf{r}) = \frac{\varepsilon_a}{4\pi} \sum_{\nu} \frac{\omega_{LT}}{\omega_{\nu} - \omega} \sum_{\mathbf{a}} \Phi_{\nu}(\mathbf{r} - \mathbf{a}) \int_{|\mathbf{r}' - \mathbf{a}| < R} \Phi_{\nu}^*(\mathbf{r}' - \mathbf{a}) \mathbf{E}(\mathbf{r}') d^3 r' \quad (8)$$

over the eigen states of the mechanical exciton in a sphere with an infinitely high barrier. Here the index $\nu = (n_r, l, m)$ characterizes the exciton state and comprises, respectively, the radial quantum number, angular momentum and its projection on the z axis, ω_{ν} is the exciton resonance frequency in the state ν . It is worthwhile to note that the functions $\Phi_{\nu}(\mathbf{r})$ satisfy Eq. (2) with $\omega = \omega_{\nu}$ and without the inhomogeneous term, i.e., with $\mathbf{E}(\mathbf{r}) \equiv 0$, they are normalized to unity and correspond to the sphere centered at the point $\mathbf{r} = 0$. The frequencies ω_{ν} are conveniently presented as $\omega_0 + (\hbar/2MR^2)x_{n_r, l}^2$, where $x_{n_r, l}$ are dimensionless numbers. For the few lowest energy levels, their values are given by π ($1s$), 4.493 ($1p$), 5.764 ($1d$), 2π ($2s$), 6.988 ($1f$), see e.g. Ref. 15, with symbols in parenthesis indicating the radial number n_r and the orbital momentum, s for $l = 0$, p for $l = 1$ etc. Note that these symbols characterize the exciton quantum-confined state whereas the internal exciton state is $1s$ all the time. Substituting the expansion (8) into the wave equation (2) and keeping in the sum over ν any one term or a finite number of terms we can study the effect of these terms on the formation of the polariton dispersion. The results are illustrated in Fig. 3. It is seen that (a) the position of the frequency $\omega_X(M)$ is mainly determined by the exciton level $1s$, (b) the polariton frequency at the X and L points is unaffected by the $1p$ level, and (c) it suffices to add the contributions from the $1d$ and $2s$ levels in order to describe quite well the position of $\omega_X(M)$ whereas, at the L point, the sum converges slowly. Obviously, this difference in the convergence is related to the choice of $P = 1.1$ in which case the effect of anticrossing near the L point is much stronger compared with that at the X point.

5. POLARITONS IN PHOTONIC CRYSTALS WITH A DIELECTRIC CONTRAST

The dashed lines 1 and 2 in Fig. 4 depict the dispersion of light waves in the vicinity of the X point of the Brillouin zone in a nonresonant photon crystal. Exactly at the X point these waves are characterized by the symmetry X_5 and $X_{5'}$. The solid lines 1', 2' and 3' show the dispersion branches calculated taking into account only the exciton-photon coupling with one excitonic level $1s$ and choosing its resonance frequency in the middle between the frequencies of the "bare" photons X_5 and $X_{5'}$. An additional branch 4' represents longitudinal exciton states which are practically dispersionless, in the following it is not discussed. Finally, the dashed-and-dotted lines 1'', 2'' illustrate the exciton-polariton dis-

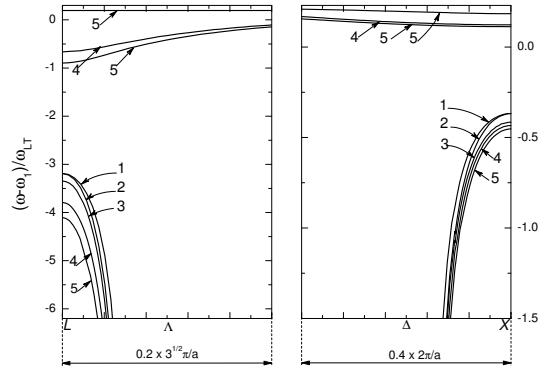


FIG. 3: Dependence of the exciton-polariton spectrum on the number of excitonic levels taken into account while calculating the dispersion curve by the Green-function technique. Lines 1, 2, 3 and 4 are obtained with allowance made, respectively, for one, two, three and four lower levels; line 5 represents the exact result taking into account all levels of exciton quantum confinement. The structure parameters used are the same as in Fig. 1.

persion with allowance made for all exciton levels. For the illustration we chose a photonic crystal with comparatively weak dielectric contrast, $\varepsilon_B = 12$, $\varepsilon_a = 13$, in order to have the lowest stop-band in the direction $\mathbf{k} \parallel [001]$, or the splitting between the X_5 and $X_{5'}$ states, comparable with the matrix element of exciton-photon interaction. It follows from Fig. 4 that the allowance for the $1s$ quantum-confined exciton states optically active in the polarization $\mathbf{E} \perp z$ results in a replacement of two branches 1, 2 by three branches 1', 2' and 3'. The addition of contributions due to other (excited) excitonic levels leads to a transformation of the branch 1' into 1'' and an appearance an extra branch 2''. Simultaneously a dense network of polariton branches is formed in the frequency region $\omega > \omega_0$. It is not shown in the figure in order to avoid overloading the image. Instead, only the exciton-polariton eigen frequencies $\omega_{\nu} > \omega_0$ at the X point are indicated by short horizontal lines intersecting the vertical line X .

In what follows we propose a two-wave approximate description of the polariton spectrum which is valid for a weak dielectric contrast and allows to understand the nature of branches indicated in Fig. 4 by primed and double-primed integers. Earlier this approximation was used in the analysis of the photon dispersion in nonresonant photonic crystals¹⁶.

The Bloch solution (4) can be expanded over the space harmonics with the wave vectors $\mathbf{k} + \mathbf{b}$. For the vec-

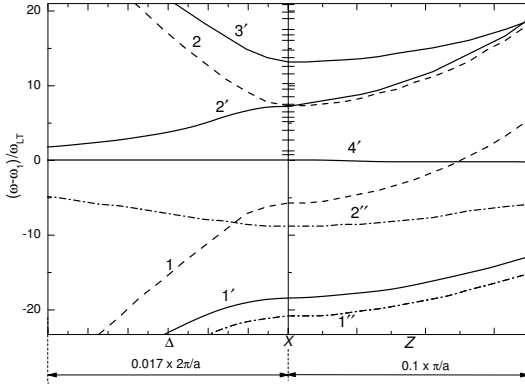


FIG. 4: Photon band structure for a crystal with the dielectric contrast, $\varepsilon_a = 12$, $\varepsilon_B = 13$. Dashed lines are calculated for a photonic crystal neglecting excitons; solid lines are obtained taking into account only the lowest excitonic level; dashed-and-dotted lines and short straight lines are obtained taking into account all quantum-confined states of the mechanical exciton.

tors $\mathbf{k} \parallel [001]$ lying close to the X point, we keep in this expansion only two terms with $\mathbf{k}_1 = (0, 0, k_1)$, $\mathbf{k}_2 = (0, 0, k_2)$ and $k_1 - k_2 = 4\pi/a$. At the X point we have $k_1 = -k_2 = 2\pi/a$. Thus, the electric field is approximated by

$$\mathbf{E}(\mathbf{r}) = \mathbf{E}_1 e^{ik_1 z} + \mathbf{E}_2 e^{ik_2 z}. \quad (9)$$

For doubly-degenerate polariton states of the Δ_5 symmetry compatible with the representations X_5 and $X_{5'}$, the amplitudes \mathbf{E}_1 and \mathbf{E}_2 are parallel to each other and perpendicular to the axis $z \parallel [001]$. Substituting Eqs. (8) and (9) into the wave equation (2), multiplying its terms by $\exp(-ik_j z)$ and integrating over the unit primitive cell $v_0 = a^3/4$ of the FCC lattice we obtain

$$[(k_1/k_0)^2 - \bar{\varepsilon}] \mathbf{E}_1 = \varepsilon' \mathbf{E}_2 + \sum_{j=1,2} \mathbf{E}_j \sum_{\nu} I_{\nu}^{(1)*} I_{\nu}^{(j)} T_{\nu}, \quad (10)$$

$$[(k_1/k_0)^2 - \varepsilon_B] \mathbf{E}_1 = [(k_2/k_0)^2 - \varepsilon_B] \mathbf{E}_2 = T_{1s} I_{1s}^2 (\mathbf{E}_1 + \mathbf{E}_2), \quad (13)$$

where I_{1s} is the integral (11) corresponding to the wave vector k_X . Provided that the frequencies ω_1 and $\omega_X \equiv ck_X/n_B$ are close to each other, the photonic states X_5 , $X_{5'}$ are replaced by three doubly-degenerate polaritonic states: one of the symmetry X_5 with the frequency ω_X and two of the symmetry $X_{5'}$ with the frequencies

$$\omega = \frac{\omega_1 + \omega_X}{2} \pm \sqrt{\left(\frac{\omega_1 - \omega_X}{2}\right)^2 + \delta^2}, \quad (14)$$

where $\delta = \sqrt{\omega_1 \omega_{LT} I_{1s}^2}$. For coinciding frequencies ω_1 and ω_X , the polariton spectrum in the direction $\mathbf{k} \parallel [001]$

$$[(k_2/k_0)^2 - \bar{\varepsilon}] \mathbf{E}_2 = \varepsilon' \mathbf{E}_1 + \sum_{j=1,2} \mathbf{E}_j \sum_{\nu} I_{\nu}^{(2)*} I_{\nu}^{(j)} T_{\nu}.$$

The notation used are as follows: $k_0 = \omega/c$,

$$\bar{\varepsilon} = \frac{1}{v_0} \int \varepsilon(\mathbf{r}) d^3 r, \quad \varepsilon' = \frac{1}{v_0} \int e^{4\pi i z/a} \varepsilon(\mathbf{r}) d^3 r,$$

$$I_{\nu}^{(j)} = \frac{1}{\sqrt{v_0}} \int e^{ik_j z} \Phi_{\nu}^*(\mathbf{r}) d^3 r, \quad T_{\nu} = \frac{\varepsilon_a \omega_{LT}}{\omega_{\nu} - \omega}, \quad (11)$$

and we assume the origin of the Cartesian coordinate system to be chosen in the center of one of the spheres A .

In the absence of the exciton-photon coupling and dielectric contrast, the right-hand sides of equations (10) vanish, $\bar{\varepsilon} = \varepsilon_B$, and we arrive at two branches of the dispersion relation (6) for “bare” photons. At the X point these branches converge. In the presence of dielectric contrast, $\varepsilon' \neq 0$ and the fourfold degenerate state at the X point splits into doubly-degenerate states $X_{5'}$ ($E_1 = E_2$) and X_5 ($E_1 = -E_2$) with their eigen frequencies being

$$\omega(X_5) = \frac{ck_X}{\sqrt{\bar{\varepsilon} - \varepsilon'}}, \quad \omega(X_{5'}) = \frac{ck_X}{\sqrt{\bar{\varepsilon} + \varepsilon'}} \quad (12)$$

and the splitting being $\omega(X_5) - \omega(X_{5'}) \approx (\varepsilon'/\bar{\varepsilon})(ck_X/\bar{n})$, where $k_X = 2\pi/a$, $\bar{n} = \sqrt{\bar{\varepsilon}}$. The approximate equations (12) reproduce with high accuracy results of the exact calculation presented in Fig. 4 by dashed lines.

In the absence of dielectric contrast, with allowance for the exciton level $1s$ only and negligible difference between the integrals $I_{1s}^{(1)}$ and $I_{1s}^{(2)}$ the set of equations (10) reduces to

has a stop-band of the width 2δ centered at $\omega = \omega_1$. The detuning of ω_X from ω_1 leads to shifts of the stop-band edges according to Eq. (13) and, in addition, an allowed band is formed in the center of the stop-band, similarly as it happens in the resonant Bragg quantum-well structure (see¹⁷ and references therein).

For an approximate description of the solid lines in Fig. 4 it suffices to keep in the sums over ν in Eqs. (10) only the contribution due to the exciton quantum-confined ground state. In this approximation the mixing of the photon and exciton states of the symmetry $X_{5'}$

leads to their repulsion and formation of hybrid waves with the frequencies

$$\omega = \frac{\omega_1 + \omega(X_{5'})}{2} \pm \sqrt{\left[\frac{\omega_1 - \omega(X_{5'})}{2}\right]^2 + \delta^2}. \quad (15)$$

The previous equation (14) is a particular case of this more general equation. Since the $1s$ quantum-confined exciton does not interact with the light wave of the symmetry X_5 , the X_5 photon frequency remains unchanged in the considered approximation. This allows to understand the closeness of the X_5 -polariton frequencies calculated neglecting the exciton effects and taking into account only the $1s$ level, see the points of intersection of the lines 2 and 2' with the vertical line X . Allowance for the excited excitonic levels in Eq. (10) results in a shift of the frequency of the lowest polariton branch $X_{5'}$ downwards (line 1''). However, their influence is small in comparison with the $1s$ exciton. At the same time, in the formation of the polariton X_5 (line 2'') the main role is played by coupling of the photon X_5 with the exciton $1p$ and $m = 0$. The calculation shows that the branch 2'' is well described by the two-wave model (10) taking into account only one excitonic state ($1p, m = 0$).

6. CONCLUSION

We have developed a theory of resonant three-dimensional photonic crystals made up of two compositional materials A (spheres) and B (dielectric matrix) for an arbitrary value of the exciton effective mass M and arbitrary dielectric contrast determined by the difference between the dielectric susceptibility ε_B of the matrix and the background dielectric constant ε_a of the material A.

For a finite value of M , the lowest polariton branch lies between the branches calculated in the two limiting cases, namely, in the absence of space dispersion, i.e., for $M \rightarrow \infty$, and with allowance for only one excitonic level, i.e., for $M \rightarrow 0$ and $\omega_1 = \text{const}$. For a satisfactory description of the polariton branches in the frequency region $\omega < \omega_1$, it suffices to take into account the light coupling with few lowest states of the mechanical exciton.

For a resonant photonic crystal with the dielectric contrast, we have analyzed the exciton-induced modification of the stop-band in the [001] direction if the exciton resonance frequency ω_1 is chosen to lie in the middle of the stop-band of the analogous photonic crystal without excitons. If the dielectric contrast is weak so that $|\varepsilon_B - \varepsilon_a| \ll \varepsilon_B$ then one can use the two-wave approximation that allows describe with good accuracy the results of numerical calculation. The main contribution into the position of the lower edge of the polariton stop-band along the $\Gamma - X$ line comes from the exciton $1s$ states interacting with the light wave of the $X_{5'}$ symmetry. The upper edge of the stop-band is governed by the coupling of the exciton ($1p, m = 0$) with the photon of the X_5 symmetry.

It should be noted that the developed theory with $M \rightarrow \infty$ can be applied for the study of photonic crystals infiltrated with dye aggregates periodically distributed in the space and characterized by a certain resonance frequency of optical transitions, see¹⁸ and references therein. The theory can be applied as well for the calculation of the dispersion of exciton-polaritons in resonant two-dimensional photonic crystals, e.g., in periodic arrays of cylinders A embedded into the matrix B.

The work is supported by the Russian Foundation for Basic Research (grant 05-02-16372) and the program of the Russian Ministry of Science and Education.

-
- ¹ E. Yablonovitch, Phys. Rev. Lett. **58**, 2059 (1987).
² S. John, Phys. Rev. Lett. **58**, 2486 (1987).
³ K.M. Ho, C.T. Chan, and C.M. Soukoulis, Phys. Rev. Lett. **65**, 3152 (1990).
⁴ R.D. Meade, A.M. Rappe, K.D. Brommer, J.D. Joannopoulos, and O.L. Alerhand, Phys. Rev. B **48**, 8434 (1993).
⁵ R. M. Hornreich, S. Shtrikman, and C. Sommers, Phys. Rev. B **49**, 10914 (1994).
⁶ J. E. Sipe, Phys. Rev. E **62**, 5672 (2000).
⁷ K. Busch, C. R. Physique **3**, 53 (2002).
⁸ O. Toader and S. John, Phys. Rev. E **70**, 46605 (2004).
⁹ K.C. Huang, E. Lidorikis, X. Jiang, J.D. Joannopoulos, K.A. Nelson, P. Bienstman, and S. Fan, Phys. Rev. B **69**, 195111 (2004).
¹⁰ E.L. Ivchenko, Y. Fu, and M. Willander, Fiz. Tverd. Tela **42**, 1705 (2000) [Phys. Solid State **42**, 1756 (2000)].
¹¹ A. Moroz, Phys. Rev. B **51**, 2068 (1995).
¹² A. Moroz, Phys. Rev. B **66**, 115109 (2002).
¹³ X. Wang, X.-G. Zhang, Q. Yu, and B.N. Harmon, Phys. Rev. B **47**, 4161 (1993).
¹⁴ H. Ajiki, T. Tsuji, K. Kawano, and K. Cho, Phys. Rev. B **66**, 245322 (2002).
¹⁵ S. Flügge, Practical quantum mechanics I, Springer-Verlag, Berlin – Heidelberg – New-York, 1971.
¹⁶ S. Satpathy, Ze Zhang, and M.R. Salehpour, Phys. Rev. Lett. **64**, 1239 (1990).
¹⁷ E.L. Ivchenko, M.M. Voronov, M.V. Erementchouk, L.I. Deych, and A.A. Lisyansky, Phys. Rev. **B70**, 195106 (2004).
¹⁸ N. Eradat, A.Y. Sivachenko, M.E. Raikh, Z.V. Vardeny A.A. Zakhidov, and R.H. Baughman, Appl. Phys. Lett. **80**, 3491 (2002).